

# FULLERENES AND BUCKYONIONS IN THE INTERSTELLAR MEDIUM

SUSANA IGLESIAS GROTH

*Instituto de Astrofísica de Canarias, E-38200 La Laguna, SPAIN*

*Departamento de Física Fundamental II, Universidad de La Laguna, E-38204 La Laguna, SPAIN*

**Abstract:** We have studied the contribution of single fullerenes and buckyonions to the interstellar extinction. The photoabsorption spectra of these molecules is predicted and compared with some of the most relevant features of interstellar extinction, the UV bump, far UV rise and the diffuse interstellar bands. We conclude that fullerenes and buckyonions may explain these features and make a preliminary estimate of the carbon fraction locked in these molecules.

## 1 Introduction

The most prominent feature in the interstellar medium extinction curve is the UV bump at 2175 Å. The carrier of this band has been frequently associated to some form of carbonaceous material (graphitic spheres, polycyclic aromatic hydrocarbons (PAHs), hydrogenated amorphous carbon, etc.) but there is no definitive conclusion on the ultimate responsible for the band. The increase in the extinction at higher energies and the existence of many much weaker diffuse interstellar bands (DIBs) in the optical [1] of unknown origin are also some of the intriguing observational properties of the interstellar material. Recently, it has been claimed the detection of fullerenes with 60-240 carbon atoms in the Allende and Murchison meteorites [2]. This is the first direct indication that fullerenes were present in the presolar nebula and strongly support previous suggestions [3] that fullerenes may exist in the interstellar medium.

In this work, we study the possible contribution of single fullerenes and buckyonions (multishell fullerenes) to the interstellar extinction. We predict their photoabsorption spectra and we compare the main features of these spectra with some of the observational properties of interstellar extinction, in particular with the characteristics of the UV bump and with the distribution of diffuse interstellar bands (DIBs) in the optical and near infrared.

## 2 General properties of fullerenes

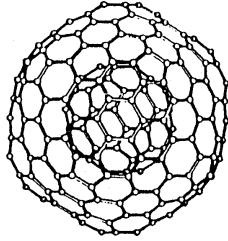


Figure 1: Buckyonion  $C_{60}@C_{240}$

The archetype of the icosahedric fullerenes is the  $C_{60}$  a closed cage formed by 60 carbon atoms distributed on the surface of a sphere of radius  $\sim 3.55 \text{ \AA}$  following the symmetry of a truncated icosahedron. In 1970, Osawa suggested that a molecule with this geometry would be chemically stable. In this molecule, each carbon atom with four valence electrons is bounded to the three nearest carbon atoms. Two of the bounds are single and link a hexagon with a pentagon, the third is double and links two hexagons. The molecule is formed then, by 30 double and 60 single bounds. The distances between atoms in single and double bounds are 1.45 and 1.37  $\text{\AA}$ , respectively. In the study of the electronic properties of the  $C_{60}$  we will consider only the four valence electrons  $2s, 2p_x, 2p_y, 2p_z$  of each carbon atom. Each of the 60 atomic orbitals  $2p_z$  is aligned in the radial direction, leading to the  $\pi$  molecular states. The three atomic orbitals  $2s, 2p_x$  y  $2p_y$  are distributed in the tangential plane to the molecular surface at the carbon atom position producing  $\sigma$  molecular states in the direction of the molecular bounds. The lineal combination of these three orbitals at each atomic site produces three hybrid orbitals  $sp^2$ , one is in the direction of the double bound and the other two are aligned with the single bounds. The 60  $\pi$  orbitals are relevant for the conductivity properties of the molecule, as in the case of graphite, and the 180  $\sigma$  orbitals are mainly responsible for the elastic properties.

The most prominent features of the empirical photoabsorption spectrum of  $C_{60}$  are two bands located at about 6 and 23 eV. These bands have been interpreted as colectiv excitations similar to the  $\pi$  and  $\sigma$  plasmon. In the fullerene  $C_{60}$  these type Mie plasmons are due to the strong delocalization of the valence electrons. The  $\sigma$ -type is much more intense than the  $\pi$ -type plasmon. It has been proposed [4] that the  $\pi$  transition could be related to the UV bump in the interstellar extinction.

## 2.1 Fullerenes with multiple spheric layers: Buckyonions

Ugarte discovered in 1991 that fullerenes can adopt multilayered configurations where one is encapsulated inside each other (see Figure 1), like onion layers [5]. In his experimental study, Ugarte used electron bombarding techniques on carbon dust using current densities of between 100 and 200  $\text{\AA}/\text{cm}^2$ . He observed the transformation of polymeric particles of carbon in others with multiple spheric layers. Diverse laboratory experiments have proven that these groups of carbon, commonly known as buckyonions can be formed by tens of layers. Electronic microscopy has determined that the separation between layers is of the order of 3.4-3.5  $\text{\AA}$ , that is approximately the separation between sheets of graphite. The buckyonions have also been synthesized exposing carbon dust to thermal treatments. Several theoretical results seem to indicate that the multilayered spheric fullerenes are the most stable form of carbon groups. Very little is known about the electronic structure of these molecules.

## 3 Fullerenes and astrophysical environments

The  $\text{C}_{60}$  molecule is obtained at high temperatures and is difficult to destroy by ultraviolet radiation or by collisions with other particles. While the other molecules have serious difficulties to survive in the interstellar medium, the robustness of  $\text{C}_{60}$  and of the other fullerenes allows their long survival. The bonds between carbon atoms make them at least as robust against dissociation in the interstellar medium as PAHs can be.

### 3.1 Meteorites

As soon as fullerenes were proposed as a form of carbon, searches in meteorites were planned. The other allotropic forms of carbon, diamonds and graphite, had been found in numerous condrites. Although at the beginning fullerenes were not detected on the Allende meteorite, more refined studies succeeded in detecting the  $\text{C}_{60}$  and  $\text{C}_{70}$  in very low densities. It is estimated that the  $\text{C}_{60}$  content of this meteorite is of 0.1 ppm. The isotopic ratios of noble gases found encapsulated in these meteoritic fullerenes are very different to the terrestrial values, supporting the theory that these molecules were not generated during the impact of the meteorite with Earth but instead were present in the original matter from which the meteorites formed. PAHs that have been proposed as precursor molecules for formation of fullerenes in the gas phase, have also been detected in meteorites. Possibly the hydrogenated form of the  $\text{C}_{60}$ , that is the  $\text{C}_{60}$  fullerane, can be found in meteorites and although little is known about which could be the properties of these hydrogenated forms in the physical circumstances and conditions of the pre- solar cloud, the presence of hydrogen in most of astrophysical contexts makes likely the conversion of fullerenes in fulleranes.

The studies of the meteorite contents of the diverse forms of carbon and its isotopic composition raise interesting questions about how these molecules could have originated. Diamonds could have been produced in the primitive pre-solar cloud at low temperatures and low pressure processes, and also in processes associated with the shock waves that may be produced in the interstellar medium as a consequence of explosions of stars or violent expulsions of mass.

### 3.2 Carbon stars and planetary nebulae

It is thought that fullerenes and graphite could originate abundantly in stellar atmospheres rich in carbon like those of some giant stars and some progenitors of planetary nebulae, objects that are characterized for important mass loss rates and therefore able to greatly enrich the interstellar medium. Carbon rich giant stars are highly evolved stars that have a greater concentration of carbon than oxygen in their atmospheres. This superficial enrichment is the consequence of nuclear reactions that take place in their interiors and of the efficient convection that transports the nucleosynthesis products to the most external layers. Carbon stars have effective temperatures in the range 2000-3000 K and are some 10,000 times brighter than the sun. They often present important mass loss rates higher, in some cases, than  $10^{-5} M_{\odot}/\text{yr}$ . The brightest stars can remain in this phase for more than  $10^5$  yr. Thus, they are an important enriching agent of carbon for the interstellar medium. In the extended envelopes surrounding these stars, a very active chemistry takes place, in particular, solid dust grains can be nucleated. These particles could grow to sizes of  $1\mu\text{m}$  although the most typical are likely of size  $0.005\mu\text{m}$  or smaller. The evidence of solid grains in the mass expelled by carbon stars comes from the continuum infrared emission much greater than expected from a photosphere. This excess of radiation is thought to be due to the emission of the circumstellar dust grains. Many carbon rich stars also present an important emission at  $11.3\mu\text{m}$  associated with solid carbon and some of them present nebulosity of reflection as a consequence of the scattering of the circumstellar grains. There are indications that in the material ejected by these stars, carbon must exist, apart from CO molecules and solid grains, in some other form or species until now unknown, fullerenes are a possibility. Unfortunately, there is very little information about the presence of molecules of intermediate size (between  $10$  and  $10^6$  atoms) in circumstellar regions. Thanks to infrared spectroscopy, it is known that there exists some bands in carbon rich planetary nebulae, for example those of  $3.3$ ,  $6.2$ ,  $7.7$ ,  $8.6$  and  $11.3\mu\text{m}$  which have not been detected in carbon stars but are observable in transition objects evolving among the giant red phase and the planetary nebula as for example, the Egg Nebula, AFGL 2688 and the Red Rectangle. These infrared bands are normally associated with the vibration modes of materials based on carbon, possibly PAHs. But until now it has not been possible to make a conclusive identification of the carrier.

### 3.3 Interstellar medium

Since the discovery of the fullerenes it has been suggested that these or particles of similar nature, could be related to one of the most intriguing problems of astrophysics: the diffuse interstellar bands discovered more than 8 decades ago, but not yet explained, and with the ultraviolet band centered in 2175 Å, which is the most intense band in the interstellar medium discovered more than 30 years ago. The origin of the UV bump is attributed to carbon particles of small size whose characteristics are not yet conclusively established. Since the 30s, it is known that there exists interstellar regions with absorption bands whose width vary between 0.5 and 50 Å. For example, between 4400 and 8900 Å, tens of these bands have been detected whose origin has not yet been clarified. They do not seem to correspond to any known spectrum of atomic or molecular origin [6]. Evidence of a relation between carbon particles and DIBs can be found in the analysis of the Red Rectangle spectrum. This object is a losing mass carbon star probably evolving to a planetary nebula phase. Diverse spectroscopic studies have revealed the good agreement between the emission lines found at 5799, 5855, 6380, and 6615 Å and some of the most intense diffuse bands of the interstellar medium. It is likely that the carrier of some of these interstellar bands is also present in the material ejected by this object.

Although the high level of symmetry of  $C_{60}$  indicates that this particular fullerene is unlikely as a carrier of the complex spectrum of the diffused interstellar bands, diverse studies have investigated possible mechanisms for which this molecule can acquire a complex spectrum of absorption in the optical. [6] already presented a model to describe the lines of resonance of several atoms (O, N, Si, Mg, Al, Na and S) trapped in the molecule of  $C_{60}$  and argued that these systems, quite stable according to laboratory tests, could be responsible for some of the DIBs. [7], suggested that the spectrum of ionized  $C_{60}$  is much more complex than the neutral molecule and could produce absorption bands in the optical and in the infrared. Foing and Ehenfreund [8] found two diffuse bands at 9577 and 9632 Å coinciding within 0.1 % with the laboratory measurements of the bands of  $C_{60}^+$  observed in a Neon mould. This was considered as evidence of the existence of the  $C_{60}^+$  in the interstellar medium. There are also several proposals associating DIBs with the hydrides of the  $C_{60}$  ( $C_{60}H_n$ ). There are also alternative suggestions that the carrier of these bands could be related to PAHs and hydrogenated amorphous carbon (HACs) compounds.

## 4 Theoretical spectra

Under some simplifications associated with the symmetry of fullerenes, it has been possible to perform [9] calculations of type Hartree-Fock in which the interelectronic correlation has been included up to second order Møller-Plesset [10, 11, 12], and calculations based on the density functional [13]. However, given the difficulties faced

by *ab initio* computations when all the electrons of these large molecules are taken into account, other semiempirical methods of the Hückel type or *tight-binding* [14] models have been developed to determine the electronic structure of  $C_{60}$  [12, 15] and associated properties like polarizabilities [16, 17], hyperpolarizabilities [18], plasmon excitations [19], etc. These semiempirical models reproduce the order of mono-electronic levels close to the Fermi level. Other more sophisticated semiempirical models, like the PPP (Pariser-Parr-Pople) [20] obtain better quantitative results when compared with photoemission experiments [21].

We have used semiempirical Hückel-type and Pariser-Parr-Pople molecular models and the random phase approximation for valence electrons to predict the electronic photoabsorption spectra of the icosahedral fullerenes  $C_{60}$ ,  $C_{240}$ ,  $C_{540}$ ,  $C_{960}$ ,  $C_{1500}$  which belong to the  $60n^2$  Goldberg family of polyhedral and for  $C_{180}$  and  $C_{720}$  which belong to the family  $20(n+1)^2$  [22]. The model parameters were first derived by fitting the available experimental photoabsorption spectrum of  $C_{60}$ , and then suitably modified to describe larger fullerenes [23, 24]. We excluded an approach based on *ab-initio* calculations for obvious practical reasons.

This study has also been extended to multishell spheric fullerenes. The microscopic electronic structure of the system is provided by an effective one-electron model and the screening effects are treated within the random phase approximation (RPA). The particular spherical geometry of these multishell fullerenes makes possible the use of electrostatic arguments to derive a simple expression for the RPA which gives the polarizability of the buckyion and the dipole moment induced on each shell in terms of either the screened or unscreened polarizabilities of the isolated shells. A systematic analysis as a function of the buckyion size has been performed [25].

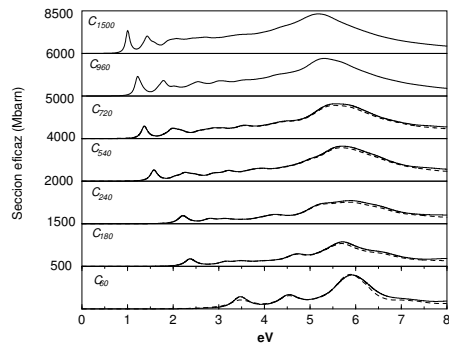


Figure 2: Photoabsorption spectra of the icosahedral fullerenes  $C_{60}$ ,  $C_{240}$ ,  $C_{540}$ ,  $C_{960}$ ,  $C_{1500}$  [23, 24]

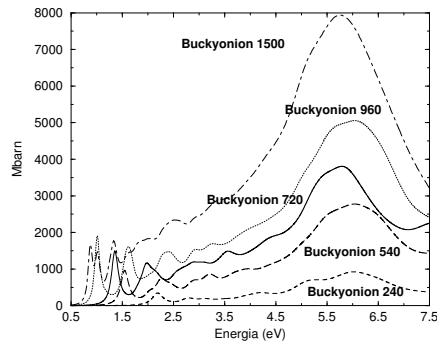


Figure 3: Photoabsorption spectra of the icosahedral buckyonions of the Goldberg family with 2, 3, 4 and 5 layers and the buckyonion  $C_{180}@C_{720}$  [24]

## 5 Interstellar extinction and the UV bump

When radiation propagates a given distance  $z$  through a medium with extinction coefficient  $\tau_{ext}(\lambda)$ , it is progressively attenuated according to the law

$$I(z) = I_0 \exp(-\tau_{ext}z) \quad (1)$$

where  $I_0$  is the intensity at the origin ( $z=0$ ). The extinction at a certain wavelength is frequently measured in magnitudes and denoted as  $A(\lambda_i)$ . The colour index of an interstellar cloud is defined as

$$E_{i-j} = A(\lambda_i) - A(\lambda_j) \quad (2)$$

The reddening factor is defined as the absorption in the V-band relative to the colour index B-V

$$R_V = \frac{A(\lambda_V)}{E_{B-V}} \quad (3)$$

This value in the diffuse interstellar medium is  $R_V \sim 3.1$  [26].

The normalized absorption at a certain wavelength  $\lambda$  also known as reddening function or extinction law can be written as

$$k(\lambda) = \frac{E_{\lambda-V}}{E_{B-V}} = \frac{A(\lambda) - A(V)}{E_{B-V}} \simeq \frac{1.086}{E_{B-V}} [\tau_{ext}(\lambda) - \tau_{ext}(V)] \quad (4)$$

It is rather usual to express the extinction law as a function of the reddening factor

Following the parameterization proposed by Fitzpatrick and Massa [26] it is possible to reproduce the extinction curves in different lines of sight in the range 3 to 8

$\mu m^{-1}$  with the function:

$$k(\lambda) = \frac{E_{\lambda-V}}{E_{B-V}} = a_1 + a_2x + a_3D(x, x_0, \gamma) + a_4F(x) \quad (5)$$

where  $x$  is energy or  $\lambda^{-1}$ . The linear component is associated to extinction by silicates and the Drude function with center in  $x_0$  and width  $\gamma$  is defined as

$$D(x, x_0, \gamma) = \frac{x^2}{(x^2 - x_0^2)^2 + \gamma^2 x^2} \quad (6)$$

Finally, the function  $F(x)$  takes into account the UV rise at energies higher than 7eV. This extinction is described

$$F(x) = 0.5392(x - x_0)^2 + 0.0564(x - x_0)^3 \quad (7)$$

The shape, wavelength and intensity of the 2175 Å band has been measured in a large number (more than 50) lines of sight [26]. It shows a profile similar to a Lorentzian or to a Drude curve [27]. The central wavelength of the bump is very stable, with changes of less than 1% from one direction to another. This small variation is, however, beyond the uncertainty of the measurements, typically smaller than 5 Å. The width of the band,  $\gamma$ , changes significantly (more than 30%) with line of sight. The average value is  $\sim 1.23$  eV ( $0.99 \mu^{-1}$ ) and the observed range is  $0.96 \leq \gamma \leq 1.5$  eV  $\mu^{-1}$  [26]. The changes in width and peak position are apparently not correlated [26]. At energies higher than 7 eV the extinction curve is similar for the various lines of sight and its intensity is not correlated with the lineal component associated to silicates, but it is weakly correlated with the height and width of the UV bump [28].

## 5.1 Theoretical spectra and the 2175 Å band

We find that, in general, the photoabsorption cross section of individual and multishell fullerenes reproduce the behaviour of the interstellar extinction curve in the near UV. Our spectra show a prominent absorption band around 5.7 eV which fits well the position and width of the 2175 Å bump. Our photoabsorption cross sections also predict an increased extinction towards higher energies (down to 1000 Å) with a shape very similar to that measured in interstellar extinction curves. The fullerenes that better reproduce the UV bump have radii in the range 7 -13 Å. Buckyonions with a complete number of shells can also reproduce the observations.

In Figures 2 and 3 the cross sections for individual and multishell fullerenes with a complete number of layers are represented. Both types of molecules suitably reproduce the peak energy and width of the interstellar band. The similarity between the theoretical cross sections and the observed extinction in the low energy range is also remarkable, we also predict here a large number of weaker bands that could be related to the DIBs.

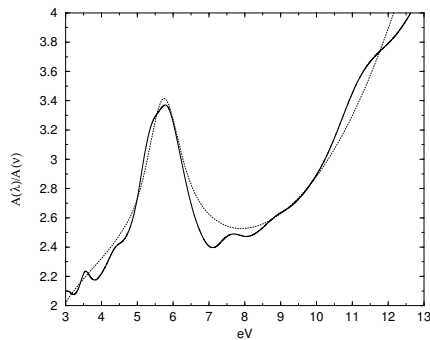


Figure 4: Photoabsorption cross section for the buckyion  $C_{180}@C_{720}$  (continuous line) compared with the interstellar extinction curve for the reddening factor  $R_V \sim 3.1$  (dashed line) [24]

## 5.2 Carbon fraction in fullerenes and buckyonions

The comparison of the computed cross sections of fullerenes and buckyonions with observations of the UV bump for  $R_V=3.1$  allow an estimate of the number of these molecules in the diffuse interstellar medium. Let us describe the extinction curve as  $a_1 + a_2x + a_3\Upsilon(x)$  where  $\Upsilon(x)$  is the theoretical cross section computed for each fullerene or buckyion. Here we assume that indeed the extinction at the energy of the bump is the result of the fullerene plus silicate contributions. We obtain via a least squared fit the relative contribution of the two components (see Figure 4). The coefficients of this lineal component do not depend significantly on the particular fullerene under consideration taking typical values of  $a_1 \simeq 1.6$  and  $a_2 \simeq 0.07$  with a relative error of 20 %.

It is known experimentally that the hydrogen column density is related with the excess colour index [29] through

$$\frac{N(H)}{E_{B-V}} = 5.9 \times 10^{21} \text{cm}^{-2} \quad (8)$$

Assuming  $A(V) \simeq 3.1E_{B-V}$  for the diffuse interstellar medium, we obtain

$$A(V) \simeq 5.3 \times 10^{-22} \text{mag cm}^2 N(H) \quad (9)$$

and the relative number density of any particular fullerene can be then estimated from the  $a_3$  coefficient

$$\frac{N(full)}{N(H)} \simeq 5 \times 10^{-22} a_3 \Upsilon(x_0) \quad (10)$$

The typical values for  $a_3$  are of order  $0.3 \times 10^{15}$  (when cross sections are expressed in barns). This coefficient changes according to the type of fullerene considered but less than 50 %, corresponding to the lowest values of the largest buckyonions. We find then that fullerenes and buckyonions may have densities in the range 0.2-0.08 particles per million (ppm) hydrogen atoms. Remarkably similar to the values found in meteorites. In the unlikely case that all types of fullerenes considered in this study had the same density in interstellar space, it would require that of order 100-200 atoms of carbon per  $10^6$  hydrogen atoms be locked in these molecules. This is a large fraction of the total carbon expected in the interstellar medium which we can assume equal to the solar atmosphere abundance of  $355 \pm 50$  [30]. It is also known from observations with the *Goddard High Resolution Spectrograph* of the Hubble telescope that in interstellar space there are  $140 \pm 20$  carbon atoms per million hydrogen atoms in gaseous form [31], therefore the maximum number of carbon atoms available for fullerenes can not be larger than 200 per million hydrogen atoms.

Indeed, the actual carbon fraction in fullerenes depend of the proper mixture of these molecules in the interstellar medium. It is likely that the number density of fullerenes and buckyonions will decrease with increasing radius (R). A distribution of the type  $N(\text{full}) \sim R^{-m}$  has been frequently considered in the literature on interstellar grain populations [32]. We have studied how a mixture of fullerenes and buckyonions following such size distribution may reproduce the observed UV bump and find that the best fits to the shape, peak energy and width of the bump are obtained for m values in the range 2.5-4.5. Such values for the power-law index lead to a lower number of carbon atoms locked in fullerenes consistent with the interstellar carbon budget. The precise determination of the actual carbon fraction requires further study and will be the subject of a forthcoming paper.

## 6 Diffuse interstellar bands

We predict that fullerenes and buckyonions, contrarily to other suggested carriers for the UV bump, display weak bands in the optical part of the spectrum. These bands populate with relatively high density this spectral range. Similar to what is seen in the diffuse interstellar bands, we find for each fullerene and buckyonion a progressive decrease of the number of transitions towards the red and infrared. Some of these bands have wavelengths consistent with known diffuse interstellar bands, reinforcing the arguments for the ubiquitous presence of these molecules in the interstellar medium.

More than 200 DIBs have been identified in the optical, most of them are found in the range 5350- 8000 Å. The stability of wavelengths and profiles suggest that the carrier of the bands is more associated with gaseous molecules than with solid grains. The widths range between 0.8 and 30 Å, thus much larger than the widths of many of

the interstellar atomic lines. The bands are not significantly polarized [33]. The most intense bands are listed in Table 1. Two DIBs at 9577 y 9632 Å have been associated to  $C_{60}^+$  [8] and a correlation has been claimed between the DIB at 4430 Å (2.8 eV) and the UV bump [34, 35].

Wavelength(Å)	W(mÅ)	Wavelength(Å)	W(mÅ)
4180	0.70	6284	1.95
4429	3.40	6533	1.89
4760	0.70	6940	0.40
4882	0.89	7429	0.56
5535	0.53	8620	0.42
5779	0.95	9577	0.50
5780	0.80	9632	0.78
6177	2.40	13170	0.40

Table 1: The most intense diffuse bands in the interstellar medium, where W is the equivalent width [1].

In Figure 5 we plot theoretical absorption bands in the optical and near infrared obtained for individual fullerenes and buckyonions. Opposite to other molecules that have been proposed as an explanation for the UV bump, fullerenes display a rich optical spectrum populated with relatively weak bands, of strength consistent with those of DIBs. Almost all the fullerenes and buckyonions considered here, present a strong band at energies close to the DIB at 4430 Å. We mark in Figure 5 the bands of fullerenes and buckyonions which have a potential DIB counterpart in the list of Herbig 1995, with a wavelength difference of less than 1%.

## 7 Formation of fullerenes and buckyonions

The mechanism of fullerene formation is only partially known [36]. They may be produced at relatively high temperatures by “annealing” of large plane monocyclic carbon molecules. Buckyonions may be produced from carbon soot and from nanodiamonds [37]. It is known that nanodiamonds of size (30-60 Å) can be transformed in particles very similar to buckyonions when heated to temperatures of 1200-1800 K [38] which are typical of carbon rich giant stars. The process may work as follows [37]: the (111) surfaces of nanodiamonds are the first to graphitize when treated at high temperature, a first graphitic layer is generated on the surface and later new concentric layers are added toward the interior in an analogous way to the process of buckyonion formation through energetic electron irradiation. Since diamond is more dense than graphite, the final particle has a larger size. Since the transformation takes

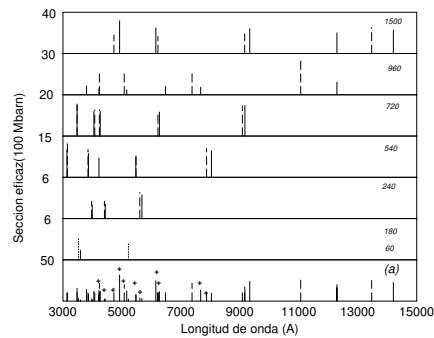


Figure 5: Comparison of the positions of weak bands in the theoretical spectrum of some fullerenes (dashed line) and buckyonions (continuous line) with known diffuse bands in the interstellar medium (crosses).

place from the surface to the interior, the final particle is of spheroidal form and very compact with the inner layer of less than  $10 \text{ \AA}$  of diameter. Nanodiamonds have been detected in meteorites [39], where they are much more abundant than graphite, and possibly in the circumstellar envelope of post-AGB stars.

## References

- [1] Herbig, G.H. 1995, *ARA&A*, 33, 19
- [2] Becker, L., Poreda, R.J., Bunch, T.E. 2000, *Lunar and Planetary Science* 31, 1803
- [3] Kroto, H.W. 1988, *Science*, 243, 1139
- [4] Braga, M., Larsson, S., Rosén, A., Volosov, A. 1991, *A&A*, 245, 232
- [5] Ugarte, D. 1992, *Nature*, 359, 707
- [6] Ballester, J.L., Antoniewicz, P.R., Smoluchowski, R. 1990, *ApJ*, 356, 507
- [7] Léger, A., d'Hendecourt, L., Verstrate, L., Schmidt, W. 1988, *A&A*, 203, 145
- [8] Foing, B.H., Ehrenfreund, P. 1994, *Nature*, 369, 296
- [9] Alasia, F., Broglia, R.A., Roman, H.E., Serra, L.L., Colo, G., Pacheco, J.M. 1994, *J. Phys. B*, 27, L643
- [10] Møller, C., Plesset, M.S. 1934, *Phys. Rev.*, 46, 618
- [11] Pople, J.A., Binkley, J.S., Seeger, R. 1976, *Int. J. Quant. Chem. Symp.*, 10, 1
- [12] Cioslowski, J. 1995, *Electronic Structure Calculations on Fullerenes and their Derivatives* (Oxford University Press, New York)
- [13] Rubio, A., Alonso, J.A., López, J.M., Stott, M.J. 1993, *Physica B*, 183, 247
- [14] Haddon, R.C. 1992, *Accounts of Chemical Research*, 25, 127

- [15] Lin, Y.L., Nori, F. 1996, *Phys. Rev. B*, 53, 1641
- [16] Bonin, K.D., Kresin, V.V. 1997, *Electric Dipole Polarizabilities of Atom, Molecules and Clusters*, World Scientific, Singapore
- [17] Ruiz, A., Hernández-Rojas, J., Bretón, J., Gómez Llorente, J.M. 1998, *J. Chem. Phys.*, 109, 3573
- [18] Fantì, M., Orlandi, G., Zerbetto, F. 1995, *J. Am. Chem. Soc.*, 117, 6101
- [19] Bertsch, G.F., Bulgac, A., Tománek, D., Wang, Y. 1991, *Phys. Rev. Lett.*, 67, 2690
- [20] Pariser, R., Parr, R.G. 1953, *J. Chem. Phys.*, 21, 466; Pariser, R., Parr, R.G. 1953, *J. Chem. Phys.*, 21, 767; Pople, J.A. 1953, *Trans. Faraday Soc*, 49, 1375
- [21] Tomanek, D., Guo, T., Jiu, C., Hauser, R.E., Chibante, L.P.F., Fure, J., Wang, L., Alford, J.M., Smalley, R.E. 1991, *J. Phys. Chem.*, 95, 7564
- [22] Yoshida, M., in <http://shachi.cochem2.tutkie.tut.ac.jp/Fuller/fsl/goldberg.html>.
- [23] Iglesias-Groth, S., Ruiz, A., Bretón, J., Gómez Llorente, J.M. 2002, *Journal of Chemical Physics*, 116, 1648
- [24] Iglesias-Groth, S. 2003, Tesis Doctoral, Universidad de La Laguna, Spain
- [25] Iglesias-Groth, S., Ruiz, A., Bretón, J., Gómez Llorente, J.M. 2003, *Journal of Chemical Physics*, 118, 7103
- [26] Fitzpatrick, E.L., Massa, D. 1986, *ApJ*, 307, 286; Fitzpatrick, E.L. 1999, *PASP*, 111, 63
- [27] Savage, B.D. 1975, *ApJ*, 199, 92
- [28] Jenniskens, P., Greenberg, J.M. 1993, *A&A*, 274, 439
- [29] Bohlin, R.C., Savage, B.D., Drake, J.F. 1978, *ApJ*, 224, 132
- [30] Grevesse, N., Noels, A. 1993, in *Origin and Evolution of the Elements*, ed. N. Prantzos, E. Vangioni-Flam and M. Cassé (Cambridge Univ. Press), p. 15
- [31] Cardelli, J.A., Meyer, D.M., Jura, M., Savage, D. 1996, *ApJ*, 467, 334
- [32] Mathis, J.S., Rumpl, W., Nordsieck, K.H. 1977, *ApJ*, 217, 425
- [33] Fahlman, G.G., Walker, G.A.H. 1975, *ApJ*, 200, 22
- [34] Nandy, K., Thompson, G.I. 1975, *MNRAS*, 173, 237
- [35] Webster, A. 1993, *MNRAS*, 265, 421
- [36] Curl, R.F., 1993 1993, *Nature*, 363, 14
- [37] Ugarte, D. 1995, *ApJ*, 443, L85
- [38] Kuznetsov, V.L., Chuvilin, A.L., Butenko, Y.V., Mal'kov, I.Y., Titov, V.M. 1994, *Chem. Phys. Letters*, 202, 343
- [39] Blake, D.F. et al. 1988, *Nature*, 332, 611